ACS OMEGA

Open Access

http://pubs.acs.org/journal/acsodf

Article

Urea–Straw–Starch Fertilizer with Tunable Water- and Nutrient-Retaining Properties Assisted by High-Energy Electron-Beam Irradiation

Chen Zhao, Jia Zhang,* Zhengyan Wu, Qiulin Yue, Lin Zhao, Shousen Guo, and Xin Zhang*

Cite This: *ACS Omega* 2023, 8, 32331–32339

Read Online

ACCESS | Metrics & More | Article Recommendations | Supporting Information

ABSTRACT: A novel type of water- and nutrient-retaining fertilizer (WNRF) was prepared by mixing, melting, and extruding high-energy electron-beam (HEEB)-irradiated corn straw, urea, and starch. HEEB irradiation technique effectively killed pathogenic microorganisms in straw and further improved the adsorption and binding capacity of straw to urea and water. Compared to nonirradiated HEEB samples, the optimal WNRF improved the water retention rate by 25.63%, the migrate-to-surface loss control rate by 60.2%, and the leaching loss control rate by 34.71%, respectively. Thus, it effectively facilitated the growth of pak choi with a 24% increase in the dry matter weight of the shoot. This work provides a promising approach to improve water and nutrient availability in arid and semi-arid regions and to promote the efficient utilization of straw resources.

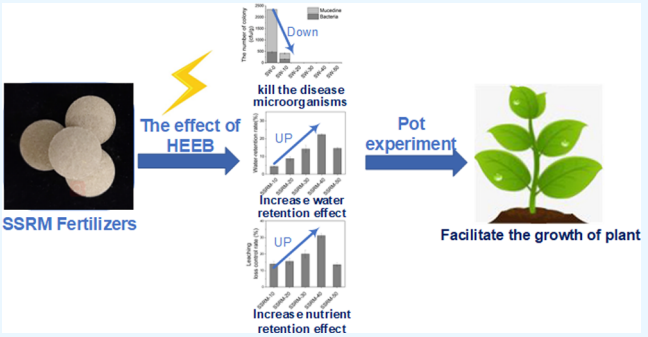

1. INTRODUCTION

According to the United Nations Population Fund (UNFPA), the world population is projected to reach 9.8 billion by 2050 due to rapid population growth.[1] However, 84% of the world's total arable land comprises arid and semi-arid regions, where crop yields are relatively low due to water scarcity and nutrition deficiencies.[2] The food crisis will intensify if relevant technologies and products are not used to improve soil quality and increase food production.[3−5]

Water- and nutrient-retaining fertilizers (WNRFs) prepared by physical adsorption,[6,7] chemical crosslinking,[8−11] and coating[12,13] can release water and fertilizer into the soil continuously and slowly, which are particularly suitable for arid and semi-arid regions,[14−18] not only to promote crop growth and yield[19] and reduce the frequency of fertilizer application[20] but also to alleviate the environmental problems of eutrophication in water bodies caused by fertilizer loss.[21,22] Most types of WNRFs incorporate chemical polymers such as polyacrylamide and polyacrylic acid to adsorb water,[23−25] but this may cause potential environmental safety problems during fertilizer production and agricultural cultivation.[26,27] Therefore, the study of WNRFs based on nontoxic biobased materials will be beneficial to protect the environment and promote the sustainable development of green agriculture.

Straw is an extremely productive but underutilized biobased material in nature. Large amounts of straw are burned directly, resulting in environmental pollution and waste of valuable biomass resources. Some straw is returned directly to the field, but it causes crop diseases and yield loss due to the presence of pathogens.[28] Corn straw has high adsorption properties and a complex grid skeleton structure consisting of cellulose (38 to 44%), hemicellulose (32 to 36%), and lignin (10 to 15%), and it also contains nitrogen, phosphorus, potassium, calcium, magnesium, and organic matter,[29] which endow it with great potential to become a base material for WNRFs. High-energy electron-beam (HEEB) irradiation is a novel physical treatment method with simple, efficient, safe, and nontoxic features, which is widely used for sterilization and modification of materials by applying a certain dose of ionizing radiation of extremely short wavelength.[30−32]

In this study, we focused on developing an environmentally friendly WNRF prepared by mixing HEEB-irradiated corn straw, starch, and urea. HEEB might effectively kill pathogens and reduce potential crop diseases caused by straw returned to the field, and the porous and loose structure formed might also improve the release control effect. This method could effectively reduce the manufacturing cost of WNRF, improve the safety performance of WNRF products, and promote the comprehensive utilization of straw.

Received: December 6, 2022
Accepted: June 27, 2023
Published: August 27, 2023

2. MATERIALS AND METHODS

2.1. Materials. Corn straw was collected from a field in Changqing (Jinan, China). Edible-grade corn starch was purchased from Yufeng Industrial Group Co. (Xingtai, China). Analytical-grade urea was purchased from Sinopharm Chemical Reagent Co. (Shanghai, China). Pak Choi "Shanghai" (*Brassica rapa subsp. chinensis*) seeds were provided by the Shandong Academy of Agricultural Sciences (Jinan, China).

2.2. Preparation of Samples. Straw powder (100−150 mesh) obtained after drying and ultrafine pulverization was irradiated with an HEEB accelerator (10 MeV and 10 kW) (Lanfu Irradiation Technology Co., Jinan, China) at room temperature at doses of 0, 10, 20, 30, 40, and 50 kGy, and the samples obtained were named SW-0, SW-10, SW-20, SW-30, SW-40, and SW-50, respectively. The above six straw materials were separately mixed with corn starch (CS) and urea (U) in the same weight ratio of 3:1:7. The resulting six mixtures were heated at 85 °C for 30 min and then pressed into WNRFs using a powder compactor (pressure 50 kN), and the resulting products were named SSRM-0, SSRM-10, SSRM-20, SSRM-30, SSRM-40, and SSRM-50, respectively.

2.3. Evaluation of Water Retention Performance. To verify the water retention performance of WNRFs, an experimental system was constructed in which 30 g of dry sand was placed in a 50 mL round-bottom centrifuge tube, followed by the slow addition of 10 mL of aqueous solutions (pH 5, 6, 7, 8, 9, or 10) of water containing 0.1 M Na_2CO_3, respectively. According to the experimental arrangement, no sample or 2 g of SSRM samples (SSRM-0, SSRM-10, SSRM-20, SSRM-30, SSRM-40, or SSRM-50) were spread on sand and then covered with 40 g of dry sand. The above systems were treated in a constant temperature incubator at 30 °C and 10% rh for 72 h and then weighed. The water retention performance of the SSRM samples was assessed by calculating the water retention rate (W_{RR}). In eq 1 for W_{RR}, the initial and time-specific weights are denoted as W_{c0} and W_{ct} for the control group and W_0 and W_t for the experimental groups, respectively.

$$W_{RR} = \frac{(W_{c0} - W_{ct}) - (W_0 - W_t)}{(W_{c0} - W_{ct})} \times 100\% \quad (1)$$

2.4. Evaluation of the Nutrient Loss Control Capacity. To verify the nutrient loss control capacity of the WNRF, experimental systems for the migrate-to-surface (MS) performance and leaching performance assessment were constructed as follows.[33]

Thirty grams of dry sand was placed in a 50 mL round-bottom centrifuge tube, 10 mL of water was slowly added, and then 2 g of urea and SSRM samples (SSRM-0, SSRM-10, SSRM-20, SSRM-30, SSRM-40, or SSRM-50) with the same urea content (2 g urea) were spread on the sand, respectively. Then, 30 g of dry sand was spread smoothly on the top. The above systems were placed in an oven at 30 °C for 24 h. Next, the top layer of sand (1 cm depth) of each treated system was taken out and transferred into a triangular flask containing 50 mL of water, shaken at 180 rpm for 40 min, and the centrifugal supernatant was collected to determine the urea concentration as the MS amount of the control group (MS_{CG}) or experimental group (MS_{EG}). The MS loss control rate (LCR_{MS}) of the SSRM sample was calculated using eq 2

$$LCR_{MS} = \frac{MS_{CG} - MS_{EG}}{MS_{CG}} \times 100\% \quad (2)$$

Thirty grams of dry sand was placed in a 50 mL round-bottom centrifuge tube with a hole (2 mm in diameter) at the bottom, and then 2 g of urea and SSRM samples (SSRM-0, SSRM-10, SSRM-20, SSRM-30, SSRM-40, or SSRM-50) with the same urea content (2 g urea) were spread on the sand, respectively. Then, 10 g of dry sand was smoothly spread on the top, followed by spraying 50 mL of water on the top layer of sand and collecting the leaching solution, where the concentration of urea was calculated as the amount of leaching loss in the control group (LL_{CG}) or experimental group (LL_{EG}). The leaching loss control rate ($LCR_{leaching}$) of each system was calculated using eq 3

$$LCR_{leaching} = \frac{LL_{CG} - LL_{EG}}{LL_{CG}} \times 100\% \quad (3)$$

2.5. Pot Trials. Pot trials of pak choi seeds were conducted in a double-glass greenhouse with temperature control (25 ± 2.5 °C) and humidification equipment (50 ± 6%). First, 1.3 kg of soil was spread on the bottom of each rectangular pot (side length, width, and depth were 45, 20, and 15 cm, respectively); then, 0.4 g of urea (as the control group) or different SSRM samples (SSRM-0, SSRM-10, SSRM-20, SSRM-30, SSRM-40, or SSRM-50) containing 0.4 g of urea (as experimental groups) were spread evenly on the surface and covered with 1.7 kg of soil, respectively. The soil (clay loam) used in the experiment was from Dehui County (Jilin, China), with a particle size of 6.0 ± 2.0 mm, moisture content of 52.5 ± 10%, organic carbon content of 20 ± 3.2%, total nitrogen of 319.3 ± 6.6 mg/kg, elemental K concentration of 272.83 ± 5.89 mg/kg, elemental P concentration of 75.42 ± 1.57 mg/kg, and pH of 5.0 ± 2.5. Eight pak choi seeds were planted in each group, and the trial period was 40 days, with 120 mL of watering every 7 days.[33]

2.6. Characterization. *2.6.1. Microbiological Count Statistics.* The nutrient agar medium consisted of 10 g/L peptone, 3 g/L beef extract, 5 g/L sodium chloride, and 20 g/L agar powder. Potato dextrose agar medium (PDA medium) was formulated by boiling 200 g of peeled potatoes cut into small strips in a pot containing 1000 mL of water for 30 min, filtering through 8 layers of gauze, adding water to a volume of 1000 mL, and then adding 20 g of glucose and 20 g of agar powder to the melt. Both the nutrient agar medium and the PDA medium were sterilized at 121 °C for 20 min.

Each SW sample (SW-0, SW-10, SW-20, SW-30, SW-40, and SW-50) was weighed, and 5 g was added to sterilized triangle flasks containing 95 g of normal saline (pre-set with the appropriate amount of glass beads in the flasks) and placed on an oscillator to shake for 30 min to dilute the liquid evenly. The above dilutions of rice straw soaking solution were separately spread on nutrient agar medium plates and PDA medium plates. The treated nutrient agar medium plates were placed in a constant temperature incubator at 37 °C for 36 h, then the number of colonies was counted, and the total number of bacteria contained in the samples was calculated accordingly. The treated PDA medium plates were placed in a constant temperature incubator at 30 °C for 72 h, then the number of colonies was counted, and the total number of mucedine contained in the samples was calculated.

2.6.2. Characterization of Material Properties. Scanning electron microscopy (SEM) (SUPRA 55, Zeiss, Germany),

https://doi.org/10.1021/acsomega.2c07787
ACS Omega 2023, 8, 32331−32339

Fourier transform infrared (FTIR) spectroscopy (Nicolet IS10, Thermo Scientific), and X-ray powder diffraction (XRD) (Empyrean, Malvern Panalytical, U.K.) were performed to collect and analyze SEM images, FTIR spectra, and X-ray spectra, respectively. Ultraviolet−visible (UV−vis) spectrophotometry (U-2910, Hitachi, Japan) was performed to determine the concentration of urea at a wavelength of 420 nm.

2.6.3. Evaluation of Plant Growth Parameters. The dry weights of the roots or shoots were weighed after treatment at 85 °C for 48 h. The total root length, mean root diameter, root surface area, root volume, and number of root tips were analyzed using ESPON perfectionV700 Photo and WinRHIZO software.

3. RESULTS AND DISCUSSION

3.1. Effect of HEEB Irradiation on Microorganisms in Straw. The presence of pathogenic microorganisms in straw is one of the main factors limiting the direct return or reuse of straw; therefore, the influence of HEEB treatment on the sterilization effect of straw was first investigated. As shown in Figure 1, the total number of microorganisms in the straw

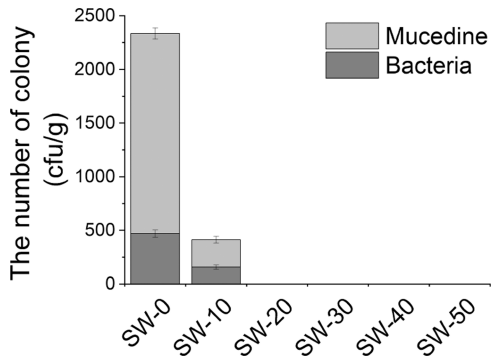

Figure 1. Effects of HEEB irradiation on the number of colonies in straw powder. SW-0, SW-10, SW-20, SW-30, SW-40, and SW-50 represent the straw powder (100−150 mesh) irradiated at 0, 10, 20, 30, 40, and 50 kGy, respectively. All experiments were repeated three times.

samples treated with irradiation doses greater than 20 kGy was almost zero, meaning that common parasitic and hemiparasitic pathogens hidden in the straw, such as *Pucciniasorghi*, *Rhizoctoniasolani*, *Fusarium gminearum*, and *Bipolarismaydis*, could be inactivated by HEEB, effectively preventing the potential biohazards associated with straw return to the field. This is because HEEB directly or indirectly destroys ribonucleic acids, proteins, and enzymes in microorganisms and even pest eggs, thus acting as a disinfectant, sterilizer, and insect repellent. Compared to traditional high-temperature and chemical disinfection methods, HEEB has the remarkable features of low energy consumption, high efficiency, safety, and nontoxicity.[34,35]

3.2. Evaluation of Water Retention Behavior. To evaluate the water retention capacity of SSRM samples, the W_{RR} of the experimental group supplemented with SSRM-0 was first compared with that of the blank control group (no sample in the water retention experimental system). As shown in Figure S1, the W_{RR} of SSRM-0 was maintained at high levels of 60−73% under pH 5−9 and high saline-alkali conditions, which might be attributed to the specificity of SSRM samples in terms of materials and the preparation process. Straw and starch had more hydrophilic groups of biobased materials; the addition of starch in the high-pressure preparation process increased the bonding ability of the materials, making straw powder and starch closely form more spatial structures and increase the hydrophilic ability of the materials. Therefore, the mixture of straw, starch, and urea could maintain a certain water retention capacity in acidic soil (pH 5.5−6.5), neutral soil (pH 6.5−7.5), and even saline-alkali soil (salinity > 0.6%).

The W_{RR} of SSRM samples treated with different irradiation doses of HEEB (as experimental groups) versus the non-irradiated material SSRM-0 (as the control group) were then measured to verify the effect of HEEB irradiation under pH 5−9 or high saline-alkali conditions. Figure 2 shows a similar trend of W_{RR} gradually increasing when the HEEB irradiation dose was 10−40 kGy, but this parameter decreased as the irradiation intensity was further increased to 50 kGy. Further analysis suggested that HEEB irradiation might affect the formation of physical rough spots or irradiation etching spots on the surface of ultrafine straw powder through direct collision, elastic scattering, and inelastic scattering, resulting in an increase in the number of pores and specific surface area of straw powder[36] to favor the adsorption and storage of water molecules. However, with further increase in the HEEB irradiation dose, the enhancement of the HEEB sputtering effect increased the number of pores in straw powder,[37] which might lead to the collapse of the pore structure, reduction of the adsorption and storage space of water molecules, and decrease of the water retention rate of SSRM-50.

The W_{RR} of the same HEEB-irradiated material also varied under different conditions; for example, the values of SSRM-40 versus SSRM-0 were 14.32, 18.35, 22.29, 25.63, 16.31, and 17.89% under pH 5−9 and high saline-alkali conditions, respectively. The straw material itself contained hydrophilic groups, such as carboxyl, carbonyl, hydroxyl, and amide groups, which could enhance the adsorption capacity of SSRM samples to water molecules. Under the conditions of high salinity or abnormal soil pH, the significantly increased ions in water could compete with water molecules for the binding site of hydrophilic groups, thus reducing the adsorption capacity of SSRM samples to water molecules and resulting in the downregulation of the water retention effect.

3.3. Evaluation of the Nutrient Loss Control Behavior. In general, due to the low humidity in arid and semi-arid areas, urea in soil tends to migrate to the surface with water evaporation and decompose into NH_3, CO_2, CH_4, and N_2O, resulting in nitrogen fertilizer loss. The LCR_{MS} is an important indicator of a WNRF. Compared to the direct application of urea (as the control group), SSRM-0 displayed a higher level of controlled release under different pH and high-salt environments (Figure S2). The LCR_{MS} values of SSRM-10 to SSRM-50 samples (as experimental groups) versus SSRM-0 indicated that HEEB irradiation from 10 to 40 kGy was beneficial in improving the controlled release capacity of sustained-release materials (Figure 3). SSRM-40 had the highest LCR_{MS} of 60.12% at pH 8 versus SSRM-0 and was 3.28 times higher than that of SSRM-10, while the LCR_{MS} of SSRM-50 was only 39.12% after exceeding the irradiation dose. This indicated that high saline-alkali and abnormal soil pH conditions reduced the positive effect of HEEB irradiation treatment.

The $LCR_{leaching}$ is also an important indicator of WNRF as arid and semi-arid areas predominantly contain sandy soils where fertilizer nutrients are susceptible to loss through leaching during irrigation and rain. In this study, the effects of

https://doi.org/10.1021/acsomega.2c07787
ACS Omega 2023, 8, 32331−32339

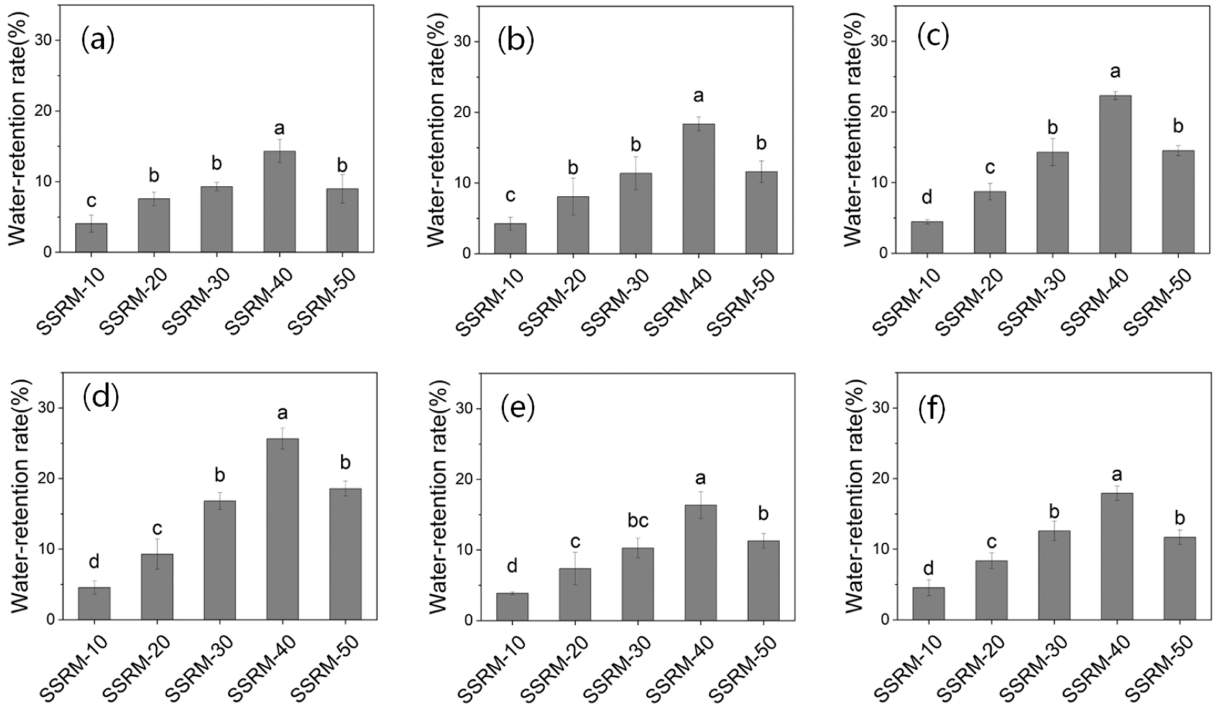

Figure 2. Water retention rate (W_{RR}) of SSRM-10 ($W_{SW\text{-}10}/W_{CS}/W_U$ = 3:1:7), SSRM-20 ($W_{SW\text{-}20}/W_{CS}/W_U$ = 3:1:7), SSRM-30 ($W_{SW\text{-}30}/W_{CS}/W_U$ = 3:1:7), SSRM-40 ($W_{SW\text{-}40}/W_{CS}/W_U$ = 3:1:7), and SSRM-50 ($W_{SW\text{-}50}/W_{CS}/W_U$ = 3:1:7) versus SSRM-0 ($W_{SW\text{-}0}/W_{CS}/W_U$ = 3:1:7) at (a) pH 5, (b) pH 6, (c) pH 7, (d) pH 8, (e) pH 9, and (f) high saline-alkali conditions (0.1 M Na_2CO_3). $W_{SW\text{-}10}$ to $W_{SW\text{-}50}$ represent the weights of different SW samples, respectively, while W_{CS} and W_U represent the weight of corn starch (CS) and urea (U), respectively. For the preparation and nomenclature of SSRM samples, refer to Section 2.2. All experiments were repeated 3 times. Different letters on the bars indicate significant difference at the 0.05 probability level.

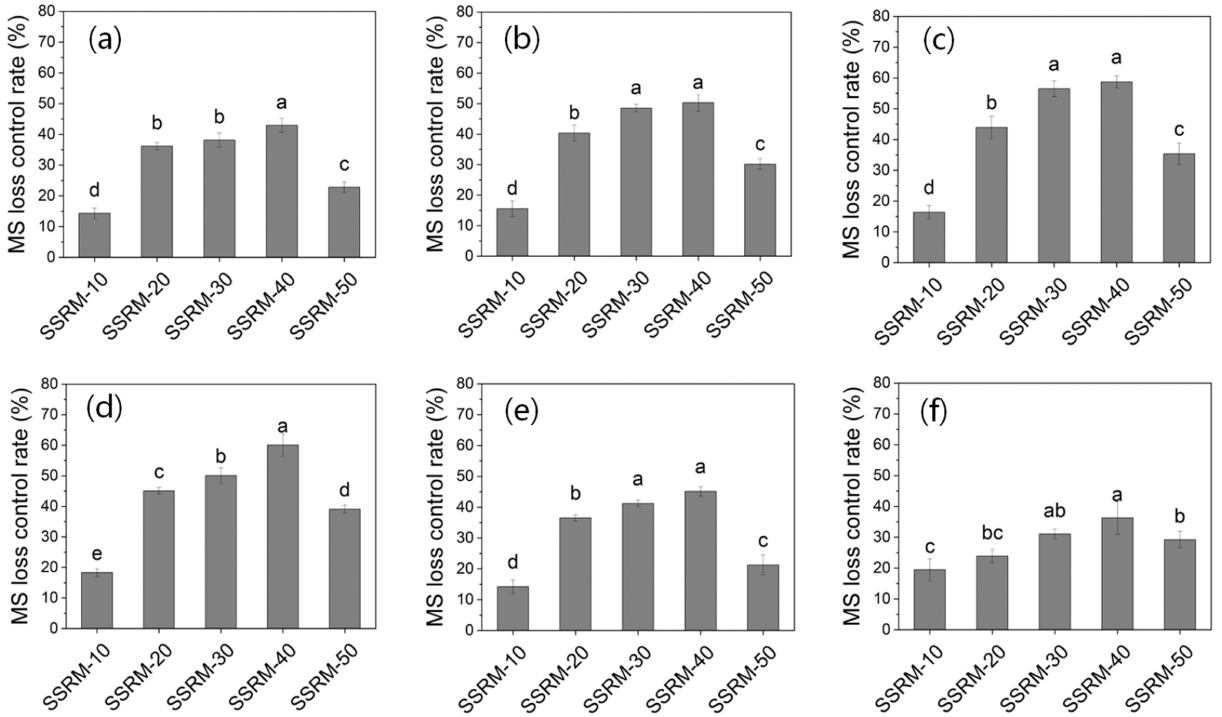

Figure 3. MS loss control rates (LCR_{MS}) of SSRM-10 ($W_{SW\text{-}10}/W_{CS}/W_U$ = 3:1:7), SSRM-20 ($W_{SW\text{-}20}/W_{CS}/W_U$ = 3:1:7), SSRM-30 ($W_{SW\text{-}30}/W_{CS}/W_U$ = 3:1:7), SSRM-40 ($W_{SW\text{-}40}/W_{CS}/W_U$ = 3:1:7), and SSRM-50 ($W_{SW\text{-}50}/W_{CS}/W_U$ = 3:1:7) relative to SSRM-0 ($W_{SW\text{-}0}/W_{CS}/W_U$ = 3:1:7) at (a) pH 5, (b) pH 6, (c) pH 7, (d) pH 8, (e) pH 9, and (f) high saline-alkali condition (0.1 M Na_2CO_3). $W_{SW\text{-}10}$ to $W_{SW\text{-}50}$ represent the weight of different SW samples, respectively, while W_{CS} and W_U represent the weight of corn starch (CS) and urea (U). For the preparation and nomenclature of SSRM samples, refer to Section 2.2. All experiments were repeated three times. Different letters on the bars indicate significant difference at the 0.05 probability level.

https://doi.org/10.1021/acsomega.2c07787
ACS Omega 2023, 8, 32331−32339

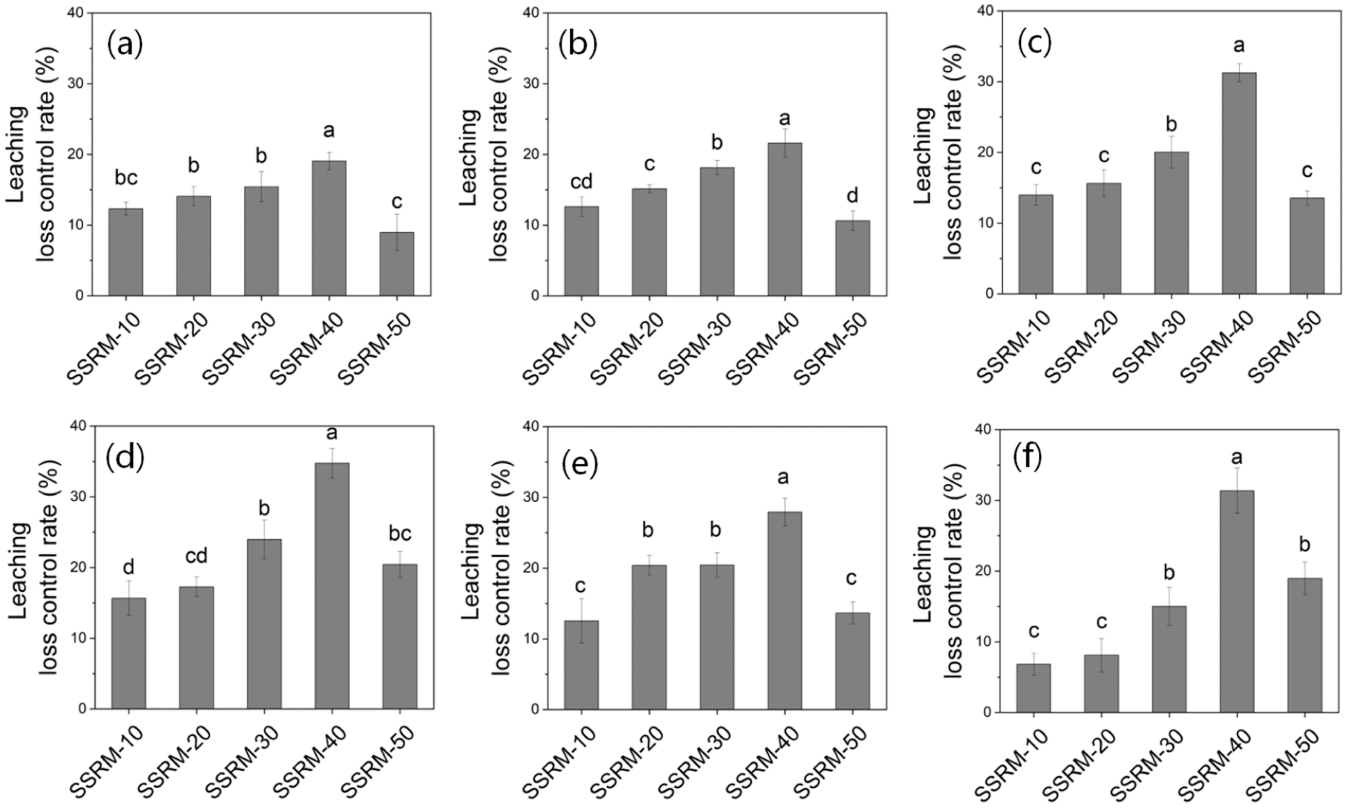

Figure 4. Leaching loss control rate ($LCR_{leaching}$) of SSRM-10 ($W_{SW\text{-}10}/W_{CS}/W_U$ = 3:1:7), SSRM-20 ($W_{SW\text{-}20}/W_{CS}/W_U$ = 3:1:7), SSRM-30 ($W_{SW\text{-}30}/W_{CS}/W_U$ = 3:1:7), SSRM-40 ($W_{SW\text{-}40}/W_{CS}/W_U$ = 3:1:7), and SSRM-50 ($W_{SW\text{-}50}/W_{CS}/W_U$ = 3:1:7) versus SSRM-0 ($W_{SW\text{-}0}/W_{CS}/W_U$ = 3:1:7) at (a) pH 5, (b) pH 6, (c) pH 7, (d) pH 8, (e) pH 9, and (f) high saline-alkali conditions (0.1 M Na_2CO_3). $W_{SW\text{-}10}$ to $W_{SW\text{-}50}$ represent the weights of different SW samples, respectively, while W_{CS} and W_U represent the weights of corn starch (CS) and urea (U), respectively. For the preparation and nomenclature of SSRM samples, refer to Section 2.2. All experiments were repeated three times. Different letters on the bars indicate significant difference at the 0.05 probability level.

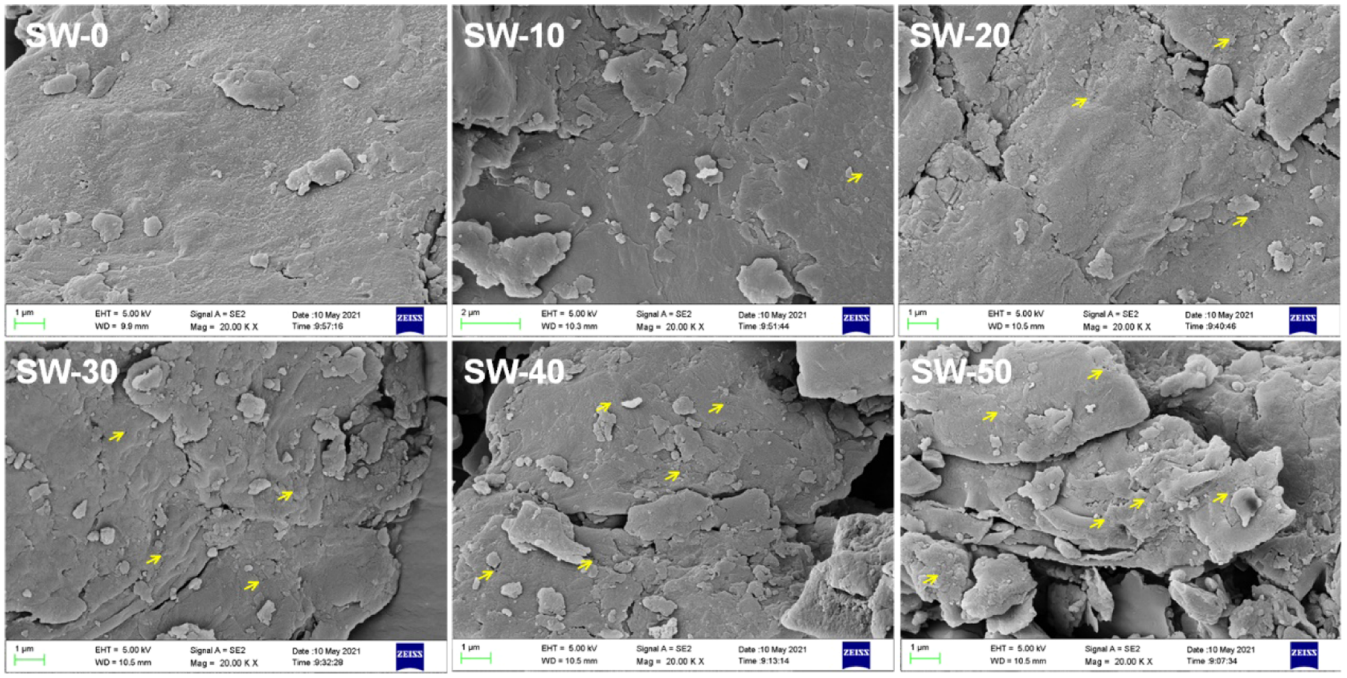

Figure 5. SEM images of SW-0, SW-10, SW-20, SW-30, SW-40, and SW-50 samples by HEEB irradiation at 0, 10, 20, 30, 40, and 50 kGy, respectively.

different pH gradients and high ionic concentrations on SSRM samples were investigated. SSRM-0 (as the experimental group) showed an excellent controlled-release performance in 0.1 M Na_2CO_3 solution at pH 5−9, with an $LCR_{leaching}$

https://doi.org/10.1021/acsomega.2c07787
ACS Omega 2023, 8, 32331−32339

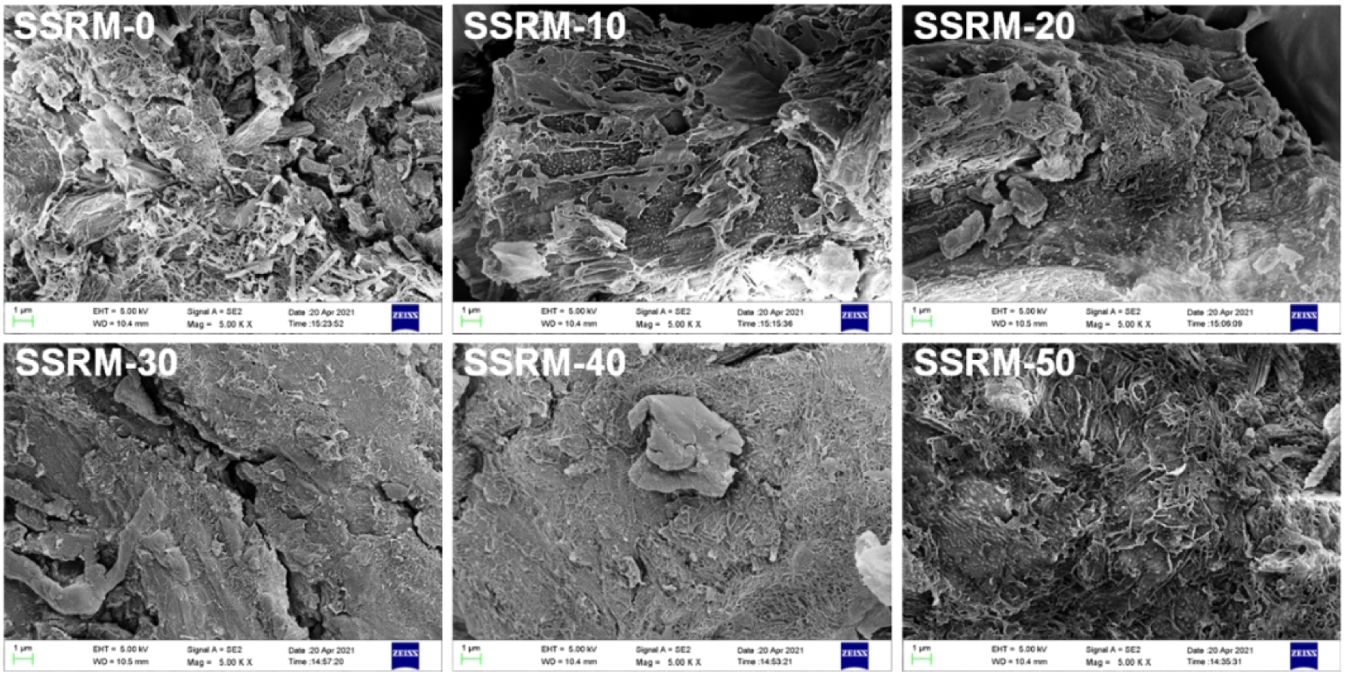

Figure 6. SEM images of SSRM-0 ($W_{SW\text{-}0}/W_{CS}/W_U$ = 3:1:7), SSRM-10 ($W_{SW\text{-}10}/W_{CS}/W_U$ = 3:1:7), SSRM-20 ($W_{SW\text{-}20}/W_{CS}/W_U$ = 3:1:7), SSRM-30 ($W_{SW\text{-}30}/W_{CS}/W_U$ = 3:1:7), SSRM-40 ($W_{SW\text{-}40}/W_{CS}/W_U$ = 3:1:7), and SSRM-50 ($W_{SW\text{-}50}/W_{CS}/W_U$ = 3:1:7). $W_{SW\text{-}0}$ to $W_{SW\text{-}50}$ respectively represent the weights of different SW samples, while W_{CS} and W_U represent the weights of corn starch (CS) and urea (U), respectively.

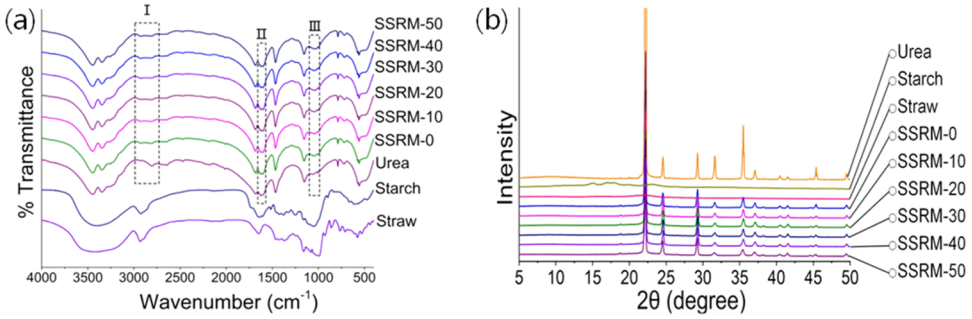

Figure 7. (a) FTIR and (b) XRD spectra of SSRM-0 ($W_{SW\text{-}0}/W_{CS}/W_U$ = 3:7:1), SSRM-10 ($W_{SW\text{-}10}/W_{CS}/W_U$ = 3:1:7), SSRM-20 ($W_{SW\text{-}20}/W_{CS}/W_U$ = 3:1:7), SSRM-30 ($W_{SW\text{-}30}/W_{CS}/W_U$ = 3:1:7), SSRM-40 ($W_{SW\text{-}40}/W_{CS}/W_U$ = 3:1:7), SSRM-50 ($W_{SW\text{-}50}/W_{CS}/W_U$ = 3:1:7), urea, straw, and starch. $W_{SW\text{-}0}$ to $W_{SW\text{-}50}$ represent the weights of different SW samples, respectively, while W_{CS} and W_U represent the weights of corn starch (CS) and urea (U), respectively. For the preparation and nomenclature of SSRM samples, refer to Section 2.2.

higher than 90% compared to that of conventional urea (as the control group) (Figure S3). Under all conditions, SSRM-10 to SSRM-50 samples (as experiment groups) exhibited higher nutrient loss control than SSRM-0 (as the control group), with SSRM-40 reaching a maximum $LCR_{leaching}$ of 34.71% at pH 8 (Figure 4), indicating that this material was suitable for application in weakly alkaline soils, such as arid and semi-arid soils.

All of the above results indicate that different HEEB irradiation intensities, pH values, and salt concentrations have similar effects on the nutrient loss control and water retention of SSRM samples. This might be attributed to the enhanced water retention capacity of SSRM, allowing it to effectively absorb the surrounding water, thus reducing the diffusion rate of urea from the composite and slowing its release. HEEB irradiation increased the specific surface area of straw powder, which enhanced the adsorption and binding capacity of water and urea. The addition of starch promoted the solidification of the powder to form particles, and the high-pressure and hot-melting treatment of SSRM samples shortened the distance between the hydrophilic groups and increased the local concentration of the groups, which facilitated the formation of the hydrophilic network structure and in turn amplified the physical effects of HEEB irradiation. However, an increase in the HEEB irradiation intensity might decrease the retarding capacity due to the collapse of the spatial structure of the materials under high pressure. Changes in pH and ion concentration might lead to changes in the binding ability of urea to groups such as carboxyl groups in straw, thus affecting the slow-release ability of SSRM samples. In summary, HEEB improved the retention performance of SSRM samples, in which SSRM-40 had the best control ability against urea loss caused by MS and leaching.

3.4. Electron Microscopy, FTIR Spectroscopy, and XRD Analysis. Electron microscopy images, as shown in Figure 5, indicated that the physical effects of HEEB resulted in a series of small pore structures appearing on the surface of straw, the number of which might gradually increase with

https://doi.org/10.1021/acsomega.2c07787
ACS Omega 2023, 8, 32331−32339

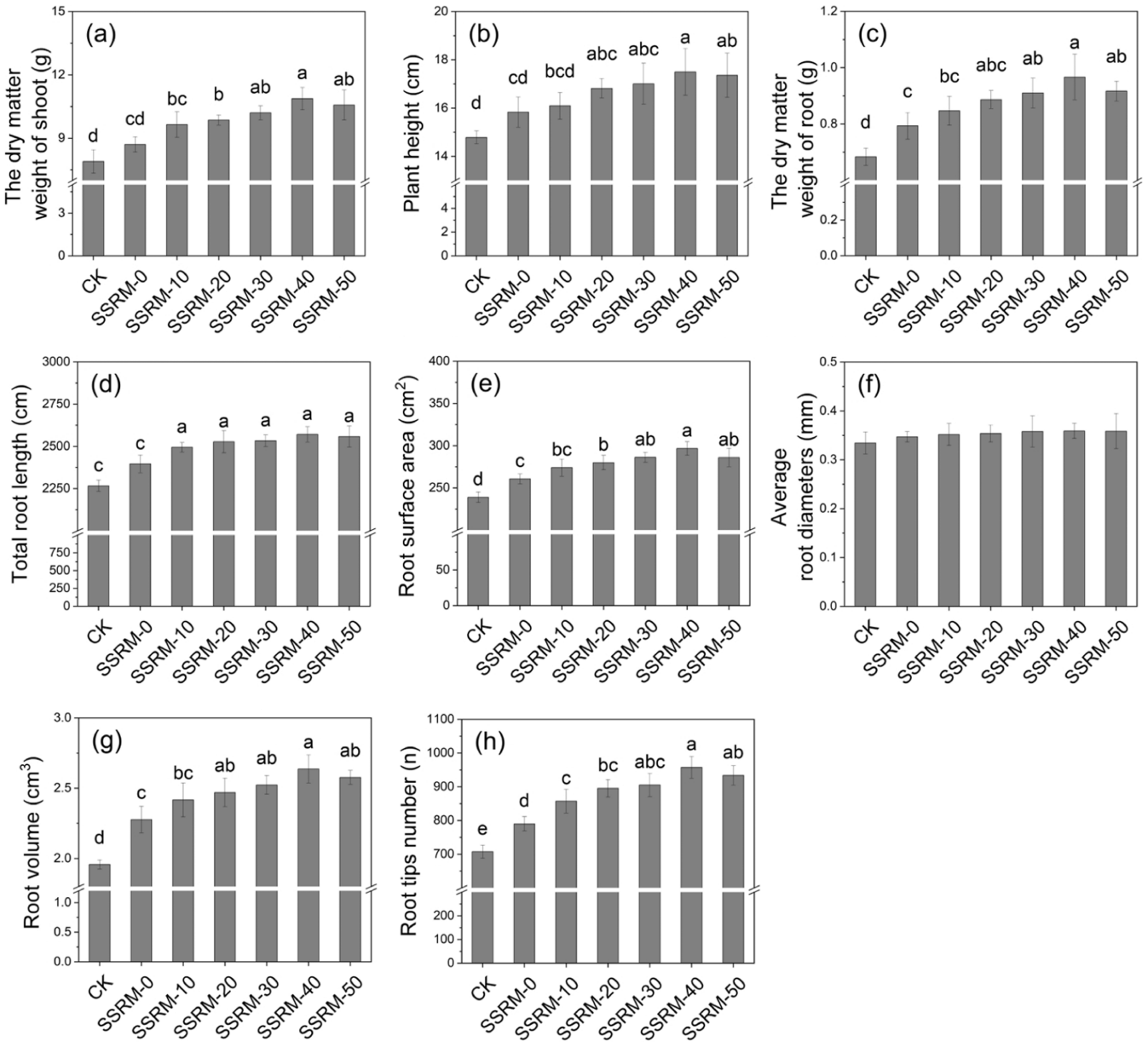

Figure 8. Effects of urea and SSRM fertilizers on the growth of pak choi according to several parameters, including (a) dry matter weight of shoot, (b) plant height, (c) dry matter weight of root, (d) total root length, (e) root surface area, (f) average root diameters, (g) root volume, and (h) root tip numbers. CK represents the control group. SSRM samples include SSRM-0 ($W_{SW\text{-}0}/W_{CS}/W_U$ = 3:7:1), SSRM-10 ($W_{SW\text{-}10}/W_{CS}/W_U$ = 3:1:7), SSRM-20 ($W_{SW\text{-}20}/W_{CS}/W_U$ = 3:1:7), SSRM-30 ($W_{SW\text{-}30}/W_{CS}/W_U$ = 3:1:7), SSRM-40 ($W_{SW\text{-}40}/W_{CS}/W_U$ = 3:1:7), and SSRM-50 ($W_{SW\text{-}50}/W_{CS}/W_U$ = 3:1:7). $W_{SW\text{-}10}$ to $W_{SW\text{-}50}$ represent the weights of different SW samples, respectively, while W_{CS} and W_U represent the weights of corn starch (CS) and urea (U), respectively. For the preparation and nomenclature of SSRM samples, refer to Section 2.2. All experiments were repeated three times. Different letters on the bars indicate significant difference at the 0.05 probability level.

increasing radiation dose, thus increasing the specific surface area and improving its capacity to retain water and nutrients. The morphology of the SSRM samples was observed by SEM and is shown in Figure 6. Compared with Figure 5, the surface of the SSRM samples was covered with urea, i.e., melted urea filled the pore structures formed by HEEB irradiation as well as the tubes and sieves of the straw itself.

To investigate the interaction in SSRM samples, FTIR measurements were performed, and the results are shown in Figure 7a. Compared with urea alone, the FTIR spectra of the SSRM series samples formed by mixing straw, starch, and urea showed certain differences in regions I, II, and III, corresponding to the characteristic peaks of 2853 cm^{-1} for the stretching vibration of C−H in the $-CH_3$ and $-CH_2-$ groups, 1637−1605 cm^{-1} for the stretching vibration of lignin-conjugated −C═O in xylogen, and 1061−1042 cm^{-1} for the stretching vibration of −C−O in cellulose or hemicellulose, indicating the successful conjugation of urea with straw and starch, respectively. In addition, the positions and intensities of the peaks of SSRM samples prepared at different HEEB irradiation doses of 0−50 kGy were similar, and no new peaks or peak shifts were found in SSRM samples compared with straw, starch, and urea.

The XRD study of the crystal structure revealed that the main diffraction peaks of urea present in the SSRM samples (22.32, 35.5, and 37.1°) were significantly weaker compared to

https://doi.org/10.1021/acsomega.2c07787
ACS Omega 2023, 8, 32331−32339

those of urea alone, as shown in Figure 7b, which is possibly due to the low crystallinity of urea in some directions after melting. Increasing the HEEB irradiation intensity did not cause significant changes in the XRD pattern, which was consistent with the preceding FTIR analysis.

The results of SEM, FTIR, and XRD analyses indicated that there was no obvious chemical reaction during the preparation of SSRM samples, including HEEB irradiation and urea melting. In other words, the preparation process of SSRM samples was primarily through the physical interaction between urea, corn straw, and starch.

3.5. Effect of SSRM on the Growth of Pak Choi. Because of the loss of fertilizers in soil, multiple applications of fertilizer are required during the growth and development of crops; otherwise, crop growth is limited at the later stage. To verify the agronomic effect of SSRM samples, pak choi was selected for a water-limited pot trial. When pak choi was transplanted, urea and SSRM samples containing the same nitrogen content were applied at once, and growth data were collected after 40 days (Figure 8). Compared to the control with urea application only, the irradiated SSRM samples showed significant differences in pak choi shoot and root dry matter weight, total root length, root surface area, root volume, and root tip numbers. The SSRM samples irradiated at doses between 30 and 50 kGy did not show significant differences in growth. SSRM-40 particularly facilitated root growth in pak choi, increasing the dry matter weight, total root length, root surface area, root volume, and root tip numbers by 41.17, 13.56, 24.37, 34.36, and 35.88%, respectively, and promoting shoot dry weight and plant height by 37.51 and 19.04%, respectively. These results indicated that SSRM-40 could effectively retain water and control urea loss, thus reducing fertilizer use and contributing to the sustainable development of green agriculture.

4. CONCLUSIONS

The HEEB-irradiated corn straw combined with urea and starch to form novel WNRFs, named SSRM samples. Compared to the nonirradiated material SSRM-0, the optimal WNRF SSRM-40 irradiated by HEEB at a dose of 40 kGy displayed a water retention rate of 25.63%, migrate-to-surface loss control rate of 60.2%, and leaching loss control rate of 34.71%. Compared with urea alone, HEEB irradiation effectively killed residual disease microorganisms in straw and significantly improved the slow release of SSRM samples, which facilitated plant root growth and yield improvement. Therefore, SSRM-40 effectively promoted the growth of pak choi with a 24% increase in the shoot dry matter weight. This WNRF achieved the resource utilization of straw, reduced the cost of fertilizer production, and could be used to improve the crop yield in arid and semi-arid areas.

ASSOCIATED CONTENT

Supporting Information

The Supporting Information is available free of charge at https://pubs.acs.org/doi/10.1021/acsomega.2c07787.

Water retention rates of SSRM-0; the MS loss control rates of SSRM-0; leaching loss control rates of SSRM-0 (PDF)

AUTHOR INFORMATION

Corresponding Authors

Jia Zhang − *Key Laboratory of High Magnetic Field and Ion Beam Physical Biology, Hefei Institutes of Physical Science, Chinese Academy of Sciences, 230031 Hefei, P. R. China;* orcid.org/0000-0002-4697-8237; Phone: +86-551-65786021; Email: zhangj@iim.ac.cn

Xin Zhang − *National Engineering Laboratory of Crop Stress Resistance Breeding, Anhui Agricultural University, 230036 Hefei, P. R. China;* orcid.org/0000-0002-9975-5088; Email: xinzhang@ahau.edu.cn

Authors

Chen Zhao − *National Engineering Laboratory of Crop Stress Resistance Breeding, Anhui Agricultural University, 230036 Hefei, P. R. China; Shandong Provincial Key Laboratory of Food and Fermentation Engineering, Shandong Food Ferment Industry Research & Design Institute, Qilu University of Technology (Shandong Academy of Sciences), 250013 Jinan, P. R. China*

Zhengyan Wu − *Key Laboratory of High Magnetic Field and Ion Beam Physical Biology, Hefei Institutes of Physical Science, Chinese Academy of Sciences, 230031 Hefei, P. R. China;* orcid.org/0000-0002-8142-1848

Qiulin Yue − *State Key Laboratory of Biobased Material and Green Papermaking, Shandong Provincial Key Laboratory of Microbial Engineering, Qilu University of Technology (Shandong Academy of Sciences), 250353 Jinan, P. R. China*

Lin Zhao − *State Key Laboratory of Biobased Material and Green Papermaking, Shandong Provincial Key Laboratory of Microbial Engineering, Qilu University of Technology (Shandong Academy of Sciences), 250353 Jinan, P. R. China;* orcid.org/0000-0002-4016-3176

Shousen Guo − *State Key Laboratory of Biobased Material and Green Papermaking, Shandong Provincial Key Laboratory of Microbial Engineering, Qilu University of Technology (Shandong Academy of Sciences), 250353 Jinan, P. R. China*

Complete contact information is available at: https://pubs.acs.org/10.1021/acsomega.2c07787

Notes

The authors declare no competing financial interest.

ACKNOWLEDGMENTS

The authors acknowledge financial support from the Shandong Provincial Natural Science Foundation (No. ZR2020QC008), the Scientific and Technological Project in Jinan (No. 202131004), the XPCC Financial Science and Technology Project in 2022 (No. 2022AB002), the Central Government Guides Local Science and Technology Development Special Fund Project (No. YDZX2021051), the Shandong Taishan Leading Talent Project (No. LJNY202015), the Major Scientific and Technological Innovation Project in Shandong Province (No. 2018CXGC0212), and the Integration of Science, Education and Industry Innovation Pilot Project of the Qilu University of Technology (No. 2020KJC-GH10).

REFERENCES

(1) Kopittke, P. M.; Menzies, N. W.; Wang, P.; McKenna, B. A.; Lombi, E. Soil and the intensification of agriculture for global food security. *Environ. Int.* **2019**, *132*, No. 105078.

(2) Carrão, H.; Naumann, G.; Barbosa, P. Mapping global patterns of drought risk: An empirical framework based on sub-national estimates of hazard, exposure and vulnerability. *Global Environ. Change* **2016**, *39*, 108−124.
(3) Al-Mamun, M. R.; Hasan, R.; Ahommed, S.; Bacchu, S.; Ali, R.; Khan, Z. H. Nanofertilizers towards sustainable agriculture and environment. *Environ. Technol. Innovation* **2021**, *23*, No. 101658.
(4) Ceccherini, G.; Duveiller, G.; Grassi, G.; Lemoine, G.; Avitabile, V.; Pilli, R.; Cescatti, A. Abrupt increase in harvested forest area over Europe after 2015. *Nature* **2020**, *583*, 72−77.
(5) Zhou, W. B.; Duan, F. Y. Closing crop yield and efficiency gaps for food security and sustainable agriculture. *J. Integr. Agric.* **2021**, *20*, 343−348.
(6) Salimi, M.; Motamedi, E.; Motesharezedeh, B.; Hosseini, H. M.; Alikhani, H. A. Starch-g-poly(acrylic acid-co-acrylamide) composites reinforced with natural char nanoparticles toward environmentally benign slow-release urea fertilizers. *J. Environ. Chem. Eng.* **2020**, *8*, No. 103765.
(7) Zhou, L. L.; Cai, D. Q.; He, L.; Zhong, N. Q.; Yu, M.; Zhang, X.; Wu, Z. Y. Fabrication of a high-performance fertilizer to control the loss of water and nutrient using micro/nano networks. *ACS Sustainable Chem. Eng.* **2015**, *3*, 645−653.
(8) Das, S. K.; Ghosh, G. K. Hydrogel-biochar composite for agricultural applications and controlled release fertilizer: a step towards pollution free environment. *Energy* **2022**, *242*, No. 122977.
(9) Huang, B. Q.; Tang, Y. J.; Zeng, Z. X.; Xue, S. M.; Ji, C. H.; Xu, Z. L. High-performance zwitterionic nanofiltration membranes fabricated via microwave-assisted grafting of betaine. *ACS Appl. Mater. Interfaces* **2020**, *12*, 35523−35531.
(10) Olad, A.; Pourkhiyabi, M.; Gharekhani, H.; Doustdar, F. Semi-IPN superabsorbent nanocomposite based on sodium alginate and montmorillonite: Reaction parameters and swelling characteristics. *Carbohydr. Polym.* **2018**, *190*, 295−306.
(11) Silva, I. A. A.; de Macedo, O. F. L.; Cunha, G. C.; Oliveira, R. V. M.; Romão, L. P. C. Using water hyacinth (*Eichhornia crassipes*) biomass and humic substances to produce urea-based multi-coated slow release fertilizer. *Cellulose* **2021**, *28*, 3691−3701.
(12) Ni, B. L.; Liu, M. Z.; Lu, S. Y. Multifunctional slow-release urea fertilizer from ethylcellulose and superabsorbent coated formulations. *Chem. Eng. J.* **2009**, *155*, 892−898.
(13) Tian, H. Y.; Li, Z. L.; Lu, P. F.; Wang, Y.; Jia, C.; Wang, H. L.; Liu, Z. G.; Zhang, M. Starch and castor oil mutually modified, cross-linked polyurethane for improving the controlled release of urea. *Carbohydr. Polym.* **2021**, *251*, No. 117060.
(14) Chen, J.; Lu, S.; Zhang, Z.; Zhao, X.; Li, X.; Ning, P.; Liu, M. Environmentally friendly fertilizers: A review of materials used and their effects on the environment. *Sci. Total Environ.* **2018**, *613-614*, 829−839.
(15) Chiaregato, C. G.; Souza, C. F.; Faez, R. The fertilizer release into water and soil as the biodegradation process in the sustainable material enhancing the fertilizer efficiency. *Environ. Technol. Innovation* **2021**, *22*, No. 101417.
(16) Li, G.-H.; Cheng, G.-H.; Lu, W.-P.; Lu, D.-L. Differences of yield and nitrogen use efficiency under different applications of slow release fertilizer in spring maize. *J. Integr. Agric.* **2021**, *20*, 554−564.
(17) Rashidzadeh, A.; Olad, A. Slow-released NPK fertilizer encapsulated by NaAlg-g-poly(AA-*co*-AAm)/MMT superabsorbent nanocomposite. *Carbohydr. Polym.* **2014**, *114*, 269−278.
(18) Zhou, T.; Wang, Y.; Huang, S.; Zhao, Y. C. Synthesis composite hydrogels from inorganic-organic hybrids based on leftover rice for environment-friendly controlled-release urea fertilizers. *Sci. Total Environ.* **2018**, *615*, 422−430.
(19) Guo, J.; Fan, J.; Xiang, Y.; Zhang, F.; Yan, S.; Zhang, X.; Zheng, J.; Hou, X.; Tang, Z.; Li, Z. Maize leaf functional responses to blending urea and slow-release nitrogen fertilizer under various drip irrigation regimes. *Agric. Water Manage.* **2022**, *262*, No. 107396.
(20) Adu-Gyamfi, R.; Agyin-Birikorang, S.; Tindjina, I.; Manu, Y.; Singh, U. Minimizing nutrient leaching from maize production systems in northern Ghana with one-time application of multi-nutrient fertilizer briquettes. *Sci. Total Environ.* **2019**, *694*, No. 133667.
(21) Naz, M. Y.; Sulaiman, S. A. Slow release coating remedy for nitrogen loss from conventional urea: a review. *J. Controlled Release* **2016**, *225*, 109−120.
(22) Wang, L.; Xin, J.; Nai, H.; Zheng, X. Effects of different fertilizer applications on nitrogen leaching losses and the response in soil microbial community structure. *Environ. Technol. Innovation* **2021**, *23*, No. 101608.
(23) Wang, J.; Chen, H.; Ma, R.; Shao, J.; Huang, S.; Liu, Y.; Jiang, Y.; Cheng, D. Novel water- and fertilizer-management strategy: Nutrient-water carrier. *J. Cleaner Prod.* **2021**, *291*, No. 125961.
(24) Wu, C. Y.; Wang, L. P.; Kang, H. T.; Dan, Y. M.; Tian, D. T.; Zheng, Y. UV-light irradiation preparation of soybean residue-based hydrogel composite from inorganic/organic hybrids for degradable slow-release N-fertilizer. *Res. Chem. Intermed.* **2020**, *46*, 1437−1451.
(25) Zaharia, A.; Radu, A. L.; Iancu, S.; Florea, A.-M.; Sandu, T.; Minca, I.; Fruth-Oprisan, V.; Teodorescu, M.; Sarbu, A.; Iordache, T.-V. Bacterial cellulose-poly(acrylic acid-co-N,N′-methylene-bis-acrylamide) interpenetrated networks for the controlled release of fertilizers. *RSC Adv.* **2018**, *8*, 17635−17644.
(26) Staples, C. A.; Murphy, S. R.; McLaughlin, J. E.; Leung, H. W.; Cascieri, T. C.; Farr, C. H. Determination of selected fate and aquatic toxicity characteristics of acrylic acid and a series of acrylic esters. *Chemosphere* **2000**, *40*, 29−38.
(27) Fujita, M.; Izato, Y.; Iizuka, Y.; Miyake, A. Thermal hazard evaluation of runaway polymerization of acrylic acid. *Process Saf. Environ. Prot.* **2019**, *129*, 339−347.
(28) Su, Y.; Yu, M.; Xi, H.; Lv, J.; Ma, Z.; Kou, C.; Shen, A. Soil microbial community shifts with long-term of different straw return in wheat-corn rotation system. *Sci. Rep.* **2020**, *10*, No. 6360.
(29) Xie, Z.; Zou, H.; Zheng, Y.; Fu, S. F. Improving anaerobic digestion of corn straw by using solid-state urea pretreatment. *Chemophere* **2022**, *293*, No. 133559.
(30) Chaudhary, N.; Singh, A.; Aswal, D. K.; Bharti, M.; Sharma, A.; Tillu, A. R.; Roy, M.; Singh, B. P.; Bahadur, J.; Putta, V.; Debnath, A. K. High energy electron beam induced improved thermoelectric properties of PEDOT: PSS films. *Polymer* **2020**, *202*, No. 122645.
(31) Gamonpilas, C.; Buathongjan, C.; Sangwan, W.; Rattanaprasert, M.; Weizman, K. C.; Klomtun, M.; Phonsatta, N.; Methacanon, P. Production of low molecular weight pectins via electron beam irradiation and their potential prebiotic functionality. *Food Hydrocolloids* **2021**, *113*, No. 106551.
(32) Aisala, H.; Nygren, H.; Seppanen-Laakso, T.; Heinio, R. L.; Kiessling, M.; Aganovic, K.; Waser, A.; Kotilainen, H.; Ritala, A. Comparison of low energy and high energy electron beam treatments on sensory and chemical properties of seeds. *Food Res. Int.* **2021**, *148*, No. 110575.
(33) Zhao, C.; Zhang, J.; Yue, Q. L.; Zhao, L.; Ma, H.; Wu, Z. Y.; Zhang, X. Itaconic acid-urea-acrylic acid copolymer as a novel water and nutrient retaining fertilizer. *Environ. Technol. Innovation* **2022**, *25*, No. 102140.
(34) Zhang, M.; Zhu, R.; Zhang, M.; Gao, B.; Sun, D.; Wang, S. High-energy pulse-electron-beam-induced molecular and cellular damage in *Saccharomyces cerevisiae*. *Res. Microbiol.* **2013**, *164*, 100−109.
(35) Wang, M.; Sun, X.; Zhong, N.; Cai, D.; Wu, Z. Promising approach for improving adhesion capacity of foliar nitrogen fertilizer. *ACS Sustainable Chem. Eng.* **2015**, *3*, 499−506.
(36) Ren, J.; Zhang, G.; Wang, D.; Cai, D.; Wu, Z. Honeycomb-like magnetic cornstalk for Cr (VI) removal and ammonium release. *Bioresour. Technol.* **2019**, *291*, No. 121856.
(37) Zhang, J.; Zhang, G.; Wang, M.; Zheng, K.; Cai, D.; Wu, Z. Reduction of aqueous CrVI using nanoscale zero-valent iron dispersed by high energy electron beam irradiation. *Nanoscale* **2013**, *5*, 9917−9923.

https://doi.org/10.1021/acsomega.2c07787
ACS Omega 2023, 8, 32331−32339